Citation for published version:
Huo, D, Wei, W & Le Blond, S 2018, 'Optimisation for interconnected energy hub system with combined ground source heat pump and borehole thermal storage', *Frontiers in Energy*, vol. 12, no. 4, pp. 529-539. https://doi.org/10.1007/s11708-018-0580-0

DOI:
10.1007/s11708-018-0580-0

Publication date:
2018

Document Version
Peer reviewed version

Frontiers in Energy
https://doi.org/10.1007/s11708-018-0580-0
RESEARCH ARTICLE

CN 11-6017/TK
ISSN 2095-1701

Optimisation for interconnected energy hub system with combined ground source heat pump and borehole thermal storage

Da HUO, Wei WEI, Simon Le BLOND
Department of Electronic & Electrical Engineering, University of Bath, Claverton Down, Bath, BA2 7AY, UK

Front. Energy., **Just Accepted Manuscript** • https://doi.org/10.1007/s11708-018-0580-0
http://journal.hep.com.cn on July 26, 2018

Verso: Front. Energy

Recto: Da HUO et al. Optimisation for interconnected energy hub system

https://doi.org/10.1007/s11708-018-0580-0

RESEARCH ARTICLE

Da HUO, Wei WEI, Simon Le BLOND

Optimisation for interconnected energy hub system with combined ground source heat pump and borehole thermal storage

Abstract Ground source heat pumps (GSHP) give zero-carbon emission heating at a residential level. However, as the heat is discharged, the temperature of the ground drops, leading to a poorer efficiency. Borehole inter-seasonal thermal storage coupled with GSHP maintains the efficiency at a high level. To adequately utilize the high performance of combined GSHP and the borehole system to further increase system efficiency and reduce cost, such a combined heating system is incorporated into the interconnected multi-carrier system to support the heat load of a community. The borehole finite element (FE) model and an equivalent borehole transfer function are proposed and respectively applied to the optimisation to analyze the variation of GSHP performance over the entire optimisation time horizon of 24 h. The results validate the borehole transfer function, and the optimisation computation time is reduced by 17 times compared with the optimisation using the FE model.

Keywords borehole thermal storage, energy hub, ground source heat pumps (GSHP), particle swarm optimisation

1 Introduction

To reduce the pollution caused by utilizing fossil fuels and adopt a sustainable economy, the UK government aims to reduce carbon emissions by 80% before 2050 compared with the 1990 baseline [1]. Domestic buildings consume 40% of the total energy of the society [2], which implies that there is a great potential for saving energy and increasing energy efficiency at domestic level. The energy hub modeling approach could, therefore, be employed to adequately exploit renewable energy, increasing energy efficiency and sustainability without compromising on energy security. The energy hub modeling frame work provides an effective way to holistically harness different energy infrastructures by considering them as an integrated system. The corresponding co-generation or tri-generation technology enables flexible energy management among all available energy carriers [3].

A typical energy hub provides the functions of importing, exporting, converting, and storing energy. Conventional converters such as gas furnace and micro-turbine have been analyzed within the energy hub system [4,5]. Recently, research efforts have been made to address the application of low-carbon and high efficiency converters in energy hub systems, such as combined heat and power plant (CHP) [6,7] and heat pumps [8]. The efficiency of the heat pump is dependent on the heat source temperature and indoor temperature. The application of the borehole storage can significantly increase the GSHP performance since the thermal storage provides a high temperature source, raising the coefficient of performance (CoP) of ground source heat pumps (GSHP). Therefore, the combination of GSHP and borehole thermal storage is studied in this paper.

Energy storage system is a viable solution for the multi-carrier system to stabilize and balance system equilibrium [9,10]. Borehole thermal storage uses the ground as a heat source and storage medium. High temperature fluid flows through the borehole pipes and stores the heat energy into the surrounding ground and this process is done by heat transfer [11]. After the

Received Dec. 23, 2017; Accept May 15, 2018; online Aug. 30, 2018

Da HUO (✉), Wei WEI, Simon Le BLOND

Department of Electronic & Electrical Engineering, University of Bath, Claverton Down, Bath, BA2 7AY, UK

Email: dh466@bath.ac.uk

fluid dumps the heat into the borehole, the temperature settles down in the borehole wall area and when the heat is needed from the borehole, the fluid extracts the heat from borehole wall and provides high temperature source. The relationship between borehole wall temperature and charging/discharging energy is analyzed by applying the finite element method which is used to synthesize an equivalent borehole wall temperature transfer function. In the FE model, the mesh number is enormous, which wastes more time. As a result, it is significant to simplify the borehole model. Borehole transfer function model uses the borehole wall temperature response to the input heat flux to create a simplified borehole model.

To sufficiently utilize the high performance of combined GSHP and borehole system to further decrease the overall system cost, the combined GSHP and borehole system operations are optimised within the context of the energy hub in this paper.

In addition to the traditional optimisation of the single energy hub, the interconnecting heterogeneous energy infrastructure at a local level can best leverage renewable generation and pooled storage without suffering from large distance transmission losses and enable self-sufficient energy communities. Additionally, the energy management between buildings enables adequate utilization of energy redundancy in each building, which comprehensively achieves the system optimisation. Hence the interconnected energy hub approach at the residential level has a huge potential for reducing the energy costs and increasing the energy efficiency. The optimisation considering both the power flow and energy hub operations within the interconnected energy hub system has been implemented in Refs. [4,7,12–14]. However, when the mathematical model of heat storage such as borehole is explicitly considered, the coordination of GSHP and heat storage within the context of energy hub optimisation has not been studied. This paper investigates the optimisation of an interconnected energy hub system with different heating converters equipped within each hubs. Such a heating network considers the effective cooperation between the conventional gas heating, CHP and a combined GSHP and borehole storage system.

To effectively reduce the cost of the energy hub system, an optimal policy needs to be determined against the time-varying energy tariffs, converter efficiency etc. The performance of GSHP at each time step is related to the wall temperature of the borehole, which is derived by analyzing the heat flux input/output from the borehole over the whole time horizon. Besides, due to the ramp rate restriction for CHP, the operations of a CHP between each time step are interdependent. Therefore, the optimisation of the interconnected energy hub system is formulated as a non-convex multi-period optimisation problem. Different approaches have been implemented to solve energy hub optimisation problems with similar complexity. In Refs. [12,15], the model predictive control scheme is applied to optimally control the operations of three interconnected energy hub systems. The multi-agent genetic algorithm is utilized to optimise the power and gas flows between energy hubs in Refs. [4,16]. The multiagent-based consensus algorithm and the event-triggered control scheme are respectively applied in Refs. [17,18] to optimise the multi-carrier system within the context of energy internet. The existence of Nash equilibrium is researched for the optimisation of multiple energy hub systems in Refs. [19–22]. A modified version of the teaching-learning-based optimisation is proposed and carried out in Ref. [5] for the energy hub system where the converters present a non-constant efficiency. Among the above optimisation techniques, the global minimum cannot be guaranteed when solving the highly-complexed problem, and the mathematical problem is relatively easy when the global minimum could be found. A decomposed approach for implementing particle swarm optimisation (PSO) [23] is proposed in Ref. [14], which presents a high performance with a fast converging speed when solving the highly-constrained interconnected energy hub problem. The decomposed technique is, therefore, utilized in this paper to optimise the operations of the energy hub system together with the borehole system.

To sum up, in this paper, the optimal operations of combined GSHP and borehole system is investigated within the optimisation scheme of energy hub, an equivalent transfer function of the borehole model is presented, and the decomposed technique of applying PSO is incorporated to the interconnected energy hub optimisation.

2 Modeling

Since domestic buildings consume approximately 40% of the total energy, in which the electricity consumption accounts for around 68% [2], the power system can significantly benefit from optimally dispatching the application of various energy carriers among residential houses. As any scale of energy systems can be modeled by energy hub [24], and different energy infrastructures such as electricity, gas, and heat are generally equipped within domestic houses, the energy hub is, therefore, applied to model the residential house. In this paper, the optimal operations of multiple residential houses with borehole system are investigated.

The configuration of K number of interconnected energy hubs is shown in Fig. 1. The system represents a community including K residential houses where electricity and heat could be shared between each other. The power adjustment between hubs could be achieved through the electrical connection indicated in Fig. 1. For example, the electricity transfer from hub K–1 to hub K is achieved by injecting electricity to the grid from hub K–1, and extracting the same amount of electricity from the grid to hub K. The heat sharing is assumed to be available between adjacent hubs. The borehole storage is set up within the community, which supplies the GSHP equipped within each house. The heating converter including micro-combined heat and power systems (micro-CHP) and gas furnace are also included. Each house is modeled as an energy hub.

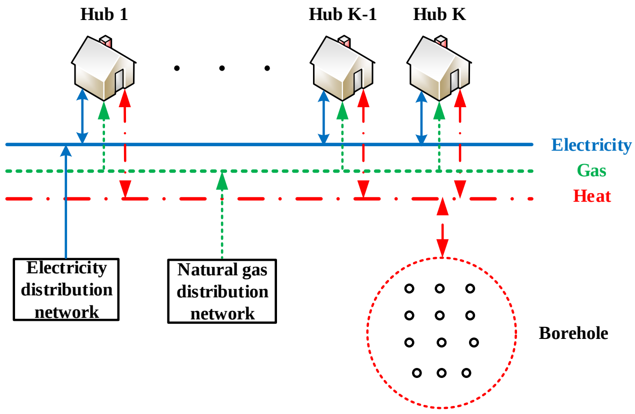

Fig. 1 Eleven interconnected energy hubs system

The optimisation for the interconnected energy hub systems is implemented by determining the operations of each hub over the whole time horizon to reach a minimum system cost, with the knowledge of the prices of energy carriers, load profile, system parameters, etc. To mathematically model the optimisation problem, detailed mathematical models of converters, borehole, and energy hub are illustrated in the following sub-sections.

2.1 Micro-CHP

The micro-CHP simultaneously generate power and heat by using gas. Compared with conventional heating converters, such as a gas furnace, micro-CHP produces a higher overall efficiency and a lower carbon emission [25]. The micro-CHP employed in the energy hub model is assumed to be steady-state with a constant electric efficiency and thermal efficiency. In addition to the constraint of maximum CHP output, the ramp rate of CHP is considered in this research and given by

$$e_{\mathrm{p}}(t-1) - e_{\mathrm{ramp}} \leq e_{\mathrm{p}}(t), (1)$$

$$e_{\mathrm{p}}(t-1) + e_{\mathrm{ramp}} \geq e_{\mathrm{p}}(t), (2)$$

where e_{p} is the power output of the micro-CHP, the variable t corresponds to the time step number in discrete time, so that any variable that is a function of time is fixed during time step t, and e_{ramp} is the micro-CHP maximum ramp rate.

2.2 Ground source heat pump

In 2014, the Renewable Heat Incentive (RHI) was launched in the UK to increase the installation of low carbon technologies [26]. Heat pumps have lower carbon emissions than the conventional heating methods such as a boiler. Ground source heat pumps (GSHP) are widely used since they have a higher and more stable CoP over other heat pump types, due to the fact that ground temperatures remain constant throughout the whole year. The definition of CoP is

$$H = \mathrm{CoP} \cdot P_{\mathrm{e}}, (3)$$

where H is the heat energy output and P_{e} is the electricity required by the heat pump.

The CoP equations for this paper is obtained from the real world project, CHOICES [27]. The CoP value depends on the condenser water outlet temperature, the evaporator inlet temperature, and the GSHP installation capacity which is the maximum heat energy that GSHP can generate. GSHP is connected to the borehole storage which will provide a higher evaporator inlet temperature. GSHP consumes electricity and generates heat energy to meet the heat demand. Within each condenser temperature category and capacity limit, the CoP value can be seen as a linear function between the GSHP cut-off temperatures.

$$\mathrm{CoP}_{\mathrm{new}} = aT + b, (4)$$

where T(°C) is the borehole wall temperature, a and b are constants. The calculation of CoP values with response to different heat pump evaporator inlet temperatures (borehole wall temperature T) at each condenser outlet temperature category is demonstrated in Table 1.

Table1 GSHP CoP Calculation

Condenser water outlet temperature /°C	CoP (T represents the evaporator inlet (borehole) temperature)
30	$0.1362 \times T + 4.8002$
35	$0.1265 \times T + 4.2335$
40	$0.1135 \times T + 3.7365$
45	$0.1002 \times T + 3.2873$
50	$0.0918 \times T + 2.8072$
55	$0.0850 \times T + 2.3483$

In this system, the GSHP is used for space heating, so that the condenser water outlet temperature is set to 55°C which is the water temperature running in the radiator in houses.

2.3 Borehole

Borehole thermal storage comprises of an array of vertical holes drilled under the ground. The depth of each borehole could be up to 100 and 50 m into the bedrock. The temperature of the soil remains steady throughout the whole year. In winter, the temperature of the soil is generally higher than the ambient air temperature which helps to create a high and stable GSHP output [28]. There are three mediums in the borehole system, antifreeze agent water, grout (backfill material), and the surrounding soil. The borehole system can be built up in the FE model and there are different input boundary conditions such as temperature, density, heat capacity, the coefficient of heat conduction, heat source (heat flux), etc. With the input information, each medium is subdivided into a massive number of meshes and the value of each mesh node is solved by the partial differential equation toolbox in the MATLAB technical computing environment.

This paper uses the borehole system from the CHOICES project with 12 boreholes to supply the community modeled by the energy hub system. The CHOICES borehole FE model generates thousands of temperature points at each time step. Table 2 lists the borehole parameters used in the FE model. In the FE model, with heat flux injection/extraction, heat transfer happens between boundaries, and the temperature of the whole area is represented by each node as is depicted in Fig. 2. The temperature rises as it gets closer to the borehole center. However, the temperatures needed in the system are the borehole wall temperatures. In the FE model, the temperature distribution across the borehole storage is represented by millions of nodes, and as a result, the borehole wall temperature is obtained by calculating the mean value of the borehole wall area nodes as the orange nodes shown in Fig. 2. After the charging period, the temperature settles in the borehole wall area, and during the heating season, the borehole wall temperature is treated as the GSHP inlet temperature. As a result, the borehole wall temperature is the key aspect of this system which is affected by the heat flux extraction during the heating season.

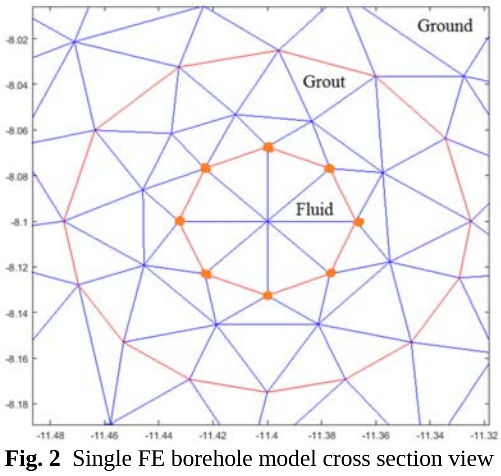

Fig. 2 Single FE borehole model cross section view

Table 2 Borehole parameters

Parameter	Ground	Grout	Fluid
Density/(kg·m^{-3})	2770	1550	1052
Heat capacity/(J·(kg·K) $^{-1}$)	826	1000	3795
Thermal conductivity/(W·(m·K)$^{-1}$)	2.61	2.1	0.5
Diameter/m	—	0.15	0.07

With the borehole wall defined, Fig. 3 gives an example of temperature response to the heat flux output. With constant heat flux (example, 1000 W/m^3) in each time step for 30 h, the borehole wall temperature decreases (as shown in Fig. 3).

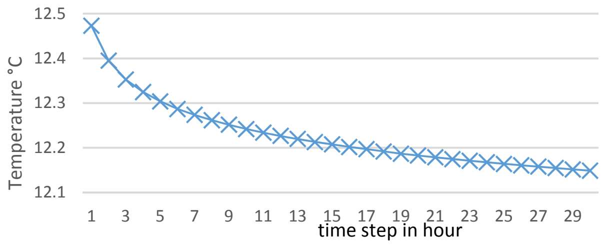

Fig. 3 Variation of borehole wall temperature with constant heat flux output

This paper focuses on the heating season so that the starting borehole wall temperature is set to an initial temperature. The borehole system is considered to be an isolated system such that the temperature exchange between the borehole unit and the far surrounding soil can be ignored due to the short simulation time. It is assumed that the borehole wall starting temperature is 20°C after the charging period which is not considered in this simulation. However, it is worth noting that in practice, the borehole wall temperature could be charged to a higher level to obtain higher CoP values over the heating season.

To accelerate optimisation, instead of using the complex borehole FE model, an equivalent borehole wall temperature transfer function is used. By using the borehole wall temperature response to the different heat flux input information from the FE model, a transfer function model is generated. It takes much less computation time for the transfer function to solve the relationship between the input heat flux and the borehole wall temperature. The transfer system is obtained by the system identification toolbox in the MATLAB using the temperature and heat flux relationship over the time.

$$H = \frac{T}{\mathrm{hf}} = \frac{8.693 \times 10^{-8}\, s + 3.625 \times 10^{-13}}{s^2 + 0.0001488s + 1.079 \times 10^{-10}}, \quad (5)$$

where T(°C) is the borehole wall temperature, hf (W/m^3) represents the heat flux, s refers to the s domain complex frequency parameter used in the transfer function.

By expressing the transfer function in the time domain, Eq. (5) can be used to model how the heat input in a previous time step leads to the temperature change in the current time step. Figure 4 exhibits the difference of borehole wall temperature change between the FE model and the transfer function with the same heat flux output over 30 h. The average temperature difference is 0.07°C, which indicates that the transfer function is accurate enough to replace the FE model for short-term optimisation.

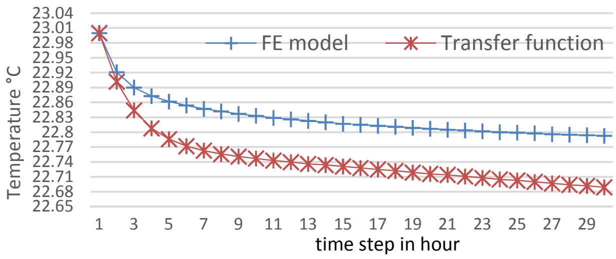

Fig. 4 Comparison of FE model and transfer function

2.4 Energy hub model

Different heating converters are equipped within the energy hub system. To efficiently analyze the system, a general formulation of energy hub model including a micro-CHP, a gas furnace, and a GSHP is proposed, as displayed in Fig. 5. The transformation between the individual hub output and input is expressed in Eq. (6).

$$\begin{bmatrix} L_{\mathrm{ele},i}(t) + E_{ij}(t) \\ L_{\mathrm{th},i}(t) + H_{ij}(t) \end{bmatrix} = \begin{bmatrix} 1 - \nu_{1,i}(t) & \nu_{2,i}(t) \times \eta_e \\ \nu_{1,i}(t) \times \mathrm{CoP}(t) & \nu_{2,i}(t) \times \eta_{\mathrm{th}} + (1 - \nu_{2,i}(t)) \times \eta_{\mathrm{gf}} \end{bmatrix} \times \begin{bmatrix} P_{\mathrm{ele},i}(t) \\ P_{\mathrm{gas},i}(t) \end{bmatrix}, (6)$$

where i and j denote the hub number; L_{ele} and L_{th} represent the electricity and heat load, respectively; P_{ele} and P_{gas} represent the power input and the gas input; η_{e} and η_{th} are the micro-CHP electric efficiency and thermal efficiency; η_{gf} is the gas furnace efficiency; v_1 is the dispatch factor, which, in this context, means the ratio of electricity injected to the heat pump divided by the total electricity input to the energy hub; v_2 denotes the ratio of gas injection to the micro-CHP compared with the total gas injection; and E_{ij} and H_{ij} indicate the power and heat import and export between hub i and other hubs.

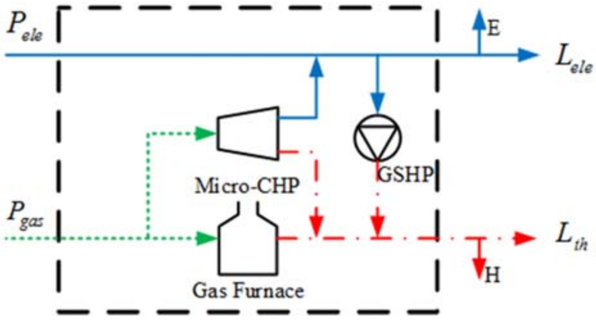

Fig. 5 Example of single energy hub

3 Problem formulation and methodology

As illustrated in Section 2, the CoP of GSHP is related to the borehole temperature, which is nonlinearly affected by the heat flux output at each time step. Additionally, the variations of borehole wall temperature over the whole optimisation time horizon are derived based on the heat flux output at every time step by using the FE model or the transfer function. Therefore, the optimisation for the system needs to be conducted by considering the operations over the whole time period, which generates a multi-period, non-convex problem. With the knowledge of load profile of the hubs, system parameters, prices of energy carriers, and system safety constraints, the optimisation is implemented for the energy hub system to minimise the energy costs over the whole time horizon. The variables to be optimised include the input of the energy carriers, the energy adjustments between hubs, the dispatch factors, and the variations of the CoPs of GSHP over the whole time horizon.

The decomposed approach of applying PSO to the complicated non-convex problem has been demonstrated to be capable of reaching a global minimum comparing with conventional algorithms with better performance [14], and hence it is applied in this paper. The problem formulation and the decomposed approach of applying PSO are illustrated in following sub-sections.

3.1 Optimisation problem formulation

The decomposed approach of utilizing PSO is applied to the interconnected energy hub system to perform an optimisation over 24 h on a typical winter day. Each hour represents one time step. The electricity load, heat load, energy price, the efficiency of each converter and the initial temperature of the borehole field at the first time step are assumed to be known. The optimisation is then implemented to determine the operation of every hub at each time to give minimum overall system costs.

However, traditional algorithms such as linear programming or other numerical methods are not capable of solving this problem. The electricity price varies between each time step. In addition, along with the variation of borehole wall temperature, the CoP of GSHP is also time dependent. Therefore, the energy hub operations at the current time step may affect the operations at other time steps. Hence, the optimisation is formulated as a multi-period problem. The efficiency of the GSHP changes at each time step, hence the problem is a non-convex optimisation problem [7]. The decomposed approach of using PSO is capable of searching the entire feasible region to find the global minimum. The optimisation is conducted in the MATLAB environment based on the ETH Zurich open source PSO code [29]. The optimisation problem is formulated as follows:

Minimize

$$\sum_{t=1}^{N}\sum_{i=1}^{K}[P_{\mathrm{ele},i}(t)\times\Pi_{\mathrm{ele}}(t)+P_{\mathrm{gas},i}(t)\times\Pi_{\mathrm{gas}}(t)].\ (7)$$

Subject to (1)–(6)

$$L_i(t)=C_i(t)\times P_i(t),\forall i,\forall t,\ (8)$$

$$0\le v_i(t)\le 1\ \forall i,\forall t.\ (9)$$

Electricity

$$P_{\mathrm{ele},i,\min}(t)\le P_{\mathrm{ele},i}(t)\le P_{\mathrm{ele},i,\max}(t),\forall i,\forall t(10)$$

$$E_{ij,\min}(t)\le E_{i,j}(t)\le E_{ij,\max}(t),\forall i,\forall t.\ (11)$$

Heat

$$H_{ij,\min}(t)\le H_{ij}(t)\le H_{ij,\max}(t),\forall i,\forall t.\ (12)$$

Gas

$$P_{\mathrm{gas},\min}(t)\le P_{\mathrm{gas},i}(t)\le P_{\mathrm{gas},\max}(t),\forall t.\ (13)$$

Heat pump

$$P_{\mathrm{HP},i,\min}(t)\le \mathrm{CoP}_i(t)\times P_{\mathrm{ele},i}(t)\times v_i(t)\le P_{\mathrm{HP},i,\max}(t),\forall i,\forall t.\ (14)$$

Gas furnace

$$P_{\mathrm{GF},\min}(t)\le P_{\mathrm{gas}}(t)\times\eta_{\mathrm{gf}}\le P_{\mathrm{GF},\max}(t),\forall t.\ (15)$$

Micro-CHP

$$e_{\mathrm{p}}(t-1)-e_{\mathrm{ramp}}\le e_{\mathrm{p}}(t)\le e_{\mathrm{p}}(t+1)+e_{\mathrm{ramp}},\forall t(16)$$

$$e_{\mathrm{p,min}}\le e_{\mathrm{p}}(t)\le e_{\mathrm{p,max}},\forall t.\ (17)$$

The control vector $u(t)$ is illustrated in Eq. (18)

$$u(t)=\left[P_{\mathrm{ele},i}(t),P_{\mathrm{gas},i}(t),E_{ij}(t),H_{ij}(t),v_i(t),\mathrm{CoP}(t)\right],\forall i,\forall t.\ (18)$$

where Π(t) denotes the energy price. Equation (8) is the energy hub transformation function corresponding to Eq. (6). N is the number of total time steps, and in this research the time step size is one hour, thus N is equal to 24. K represents the number of energy hubs modeled in the community. Equation (9) indicates the limitation for dispatch factors, and Eqs. (10) and (13) denote the minimum and maximum energy input to each hub. Equations (11) and (12) illustrate the adjustment of energy transmission limitation between hubs. Equations (14), (15), and (17) indicate the minimum and maximum power output of each converter. Equation (16) specifies the ramp rate for micro-CHP. The optimisation is carried out by determining the control vector shown in Eq. (18), which contains the power and gas inputs, the energy adjustments between hubs, the dispatch factors within all hubs, and the CoP of GSHP at all time steps.

3.2 Decomposed PSO

The concept of PSO is proposed based on the behavior of flocking birds or fish schools. Each particle represents a solution to the problem, and the fitness score of the particle denotes the performance of the particle. The group of particles updates at each iteration toward the global minimum based on the two factors of best particle ever achieved P_i^g and the best position of particle iP_i^k. The updating of all particles follows the mechanism as follows.

For particle i at iteration $k+1$, the position X is indicated as shown in Eq. (19).

$$X_i^{k+1}=X_i^k+V_i^{k+1},$$

where V_i^{k+1} means the velocity of particle i at iteration $k+1$, which is derived in Eq. (20).

where ω, c_1 , and c_2 are coefficients, r_1 and r_2 indicate two random numbers between 0 and 1. The decomposed approach of utilizing PSO to solve Eqs. (7)–(18) is illustrated in Fig. 6 based on the equations above.

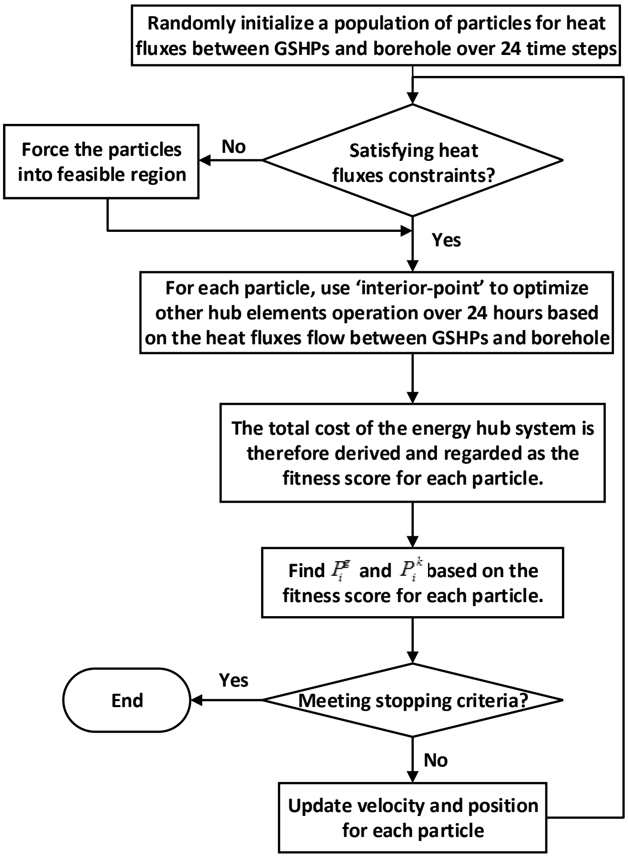

Fig. 6 Working flow of the decomposed technique of applying PSO

Equation (7) represents a highly-constrained non-convex optimisation problem. The decomposed PSO decouples the complicated problem into sub-problems, namely the scheduling of heat fluxes between GSHPs and borehole, and other elements of the interconnected energy hub system. As shown in Fig. 5, the information of heat fluxes over the whole time horizon is initialised and contained in each particle, and all particles are forced into the feasible region. The numerical method of the 'interior-point' method is then applied to optimise other hub elements over the whole time horizon based on heat fluxes information, and the total cost of the system can be derived and regarded as the fitness score for each particle. All particles update according to Eqs. (19) and (20) until the stopping criteria are met.

4 Case studies and results

4.1 System setup

Case studies are conducted for a community including 11 houses. The borehole storage is set up within the community, which supplies the GSHP equipped within houses 1, 3, 4, 6, 8, 10, and 11. The micro-CHP and gas furnace are included in houses 2 and 5, and 7 and 9 respectively. The electricity load and heat load for the 11 hubs over 24 h are generated based on Refs. [30,31], and it is assumed that the customer behaviors of the 11 houses are different, and hence the energy load profiles are various. The specific energy consumptions over the whole time horizon of hub 1 are shown in Fig. 7 as an example, in which the electricity peak loads appear at around 17:00, and the heat peak loads are at approximately 9:00 and 20:00. The efficiencies of hub devices are derived from Refs. [5,6,25]. The varying electricity price over the 24 h is obtained from Ref. [32] and shown in Fig. 8. Other parameters simulated in this paper are given in Table 3.

Table 3 Parameters for 11 hubs

Parameter	Value
e_{ramp}/(kW·min^{-1})	0.15
e_p/kW	0–0.3
η_{gf}	0.75
η_e	0.3
Π_{gas}/£	0.04
H_{th}	0.57
P_{HP}/kW	0–8.3

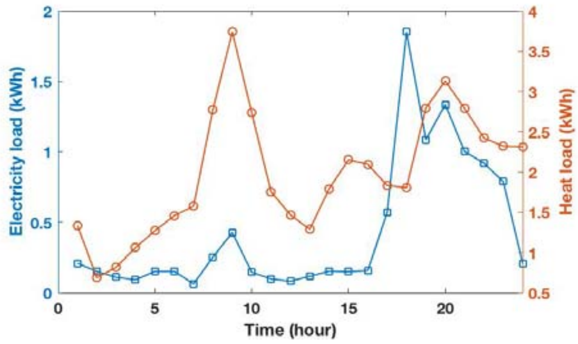

Fig. 7 Energy consumptions of hub 1 over 24 h

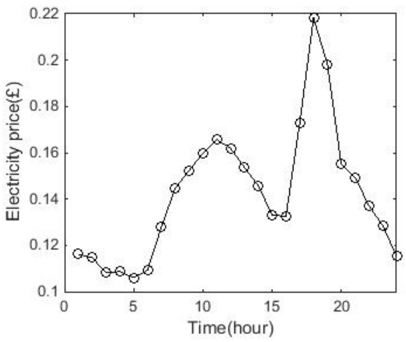

Fig. 8 Variant electricity prices against time

Four cases are presented and optimised in this paper. It is assumed that both the four cases are carried out to optimise the 11-hub system. The electricity and heat loads, system constraints, system parameters including converters efficiencies, borehole model, and the prices of the energy carriers of the four cases are the same. Comparing with using the FE model to calculate the borehole wall temperature, a transfer function model is proposed in this paper. The FE model is applied in Cases 1 and 3, and the transfer function model is applied in Cases 2 and 4 respectively. The related results are discussed to investigate the accuracy of applying the transfer function model in energy hub optimisation. To examine the benefits from interconnecting energy hubs, it is assumed that there is no power or heat connection between hubs for Cases 1 and 2, all hubs are directly connected with the grid, and the heat load in each hub is satisfied by applying its own heating converter. The energy sharing is available as indicated in Fig. 1 for Cases 3 and 4.

4.2 Convergence analysis

To demonstrate that the decomposed PSO is capable of converging to a near-global point, an optimisation is performed for the 11-hub community where the FE model for calculating the borehole wall temperature is utilized. Under the conservative stall generations (30) and stall tolerance settings (£0.0001), a population of 40 particles is utilized to implement the optimisation. The value of the objective function at each iteration is indicated in Fig. 9. It could be derived that the best particle achieves the value of £42.12 when all particles are initially generated. The optimisation result rapidly drops from iteration 1 to 44, and trends to be flat after iteration 45. The optimisation eventually converges to £37.17 after 132 iterations, which demonstrates that the application of the decomposed PSO enables a near-global minimum when solving the optimisation problem proposed in this paper.

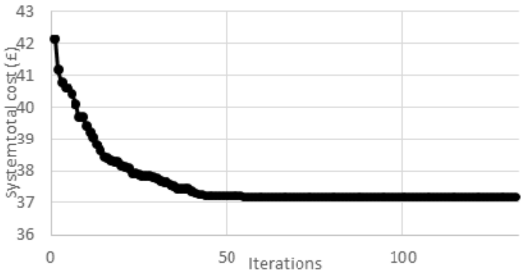

Fig. 9 Convergence behavior for the decomposed PSO applying to Case 3

4.3 Results and analysis

The total energy cost over the 24 h for each case is shown in Table 4.

Table 4 Energy cost for each case

Case number	Energy cost/£	Computation time/s
1	39.32	N/A
2	39.36	N/A
3	37.16	5998
4	37.30	248

As shown in Table 4, when the energy sharing is available between hubs, the 11-hub energy cost can be reduced by £2.16 and £2.06 respectively for the FE model and the transfer function model being employed during the optimisation. It can also be concluded that although the FE model is more accurate to estimate the borehole wall temperature, the transfer function model can achieve the results within an acceptable error (0.38%), and the computation time can be reduced by a factor of 17.

The CoP of GSHP located at each individual residential house at each time step in terms of the four cases is shown in Fig. 10. Since the CoP of GSHP is linearly correlated with the borehole wall temperature as indicated in Eq. (4), and both the FE model and transfer function model are applied to derive the borehole wall temperature, hence the differences of CoPs between Cases 3 and 4 reflect the accuracy of applying the two models. As seen from Fig. 10, the CoPs over the 24 h differ in Cases 3 and 4, but have similar variations where the CoPs difference at each time step is less than 0.01. This demonstrates that the transfer function model is capable of deriving the borehole wall temperature for energy hub optimisation over the 24 h with tiny errors.

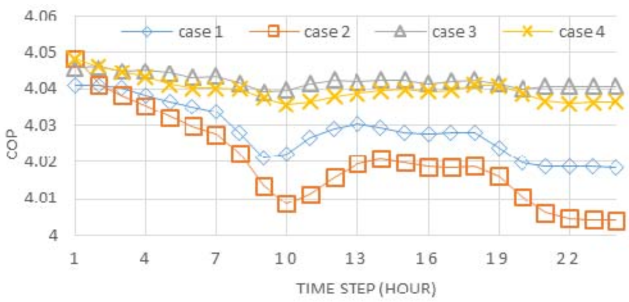

Fig. 10 CoP for GSHP over 24 h for each case

Compared with the cases that there are energy sharing between hubs, the CoP of GSHPs over the 24 h obtained from Cases 1 and 2 has a greater variation. Especially the CoP varies between the boundary of 4 and 4.05 for Case 2. Conversely, when the energy hubs are interconnected, the CoP derived from Cases 3 and 4 has a similar variation. This demonstrates that the operations of combined GSHP and borehole system tends to be more stable when the energy sharing between hubs is available.

Since the electricity price reaches the peak value around the time steps of 17 and 18, it can be seen from Fig. 10 that for optimisation Cases 3 and 4, the CoP does not drop around the high-electricity price period, which means the utilization of GSHP is accordingly reduced. Alternatively, other heating devices are activated to support the heat load.

It can also be derived from Fig. 10 that, according to the Second Law of Thermal Dynamics, when the heat is extracted from the borehole, the borehole wall temperature decreases, which generates a high temperature gradient between the wall and the surrounding storage volume. As a result, the heat replenishment from the surrounding volume to the wall occurs. When this is greater than the heat extraction from the GSHP, it will lead to a rise in temperature of the borehole wall, which explains the slight increase in the CoP value seen in Fig. 10 in the time steps of 10–14.

The total electricity injection to the 11-hub system over the 24 h is depicted in Fig. 11. Compared with Cases 1 and 2 where no energy sharing or optimisation is carried out, the electricity consumption in Cases 3 and 4 are reduced at every time step, especially during the peak price period. The reason for this is that the micro-CHP is operated during this period, and thus the generated power and heat could be exported to other hubs, avoiding the need for grid import. Meanwhile, the gas furnace is switched on to supply most of the heating instead of electricity driven GSHP in this period.

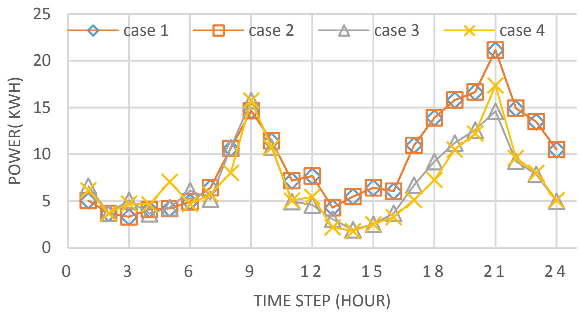

Fig. 11 Total electricity injection to 11-hub system over 24 hours for each case

5 Conclusions and future work

This paper presents the optimisation for an interconnected energy hub system including a combined GSHP and a borehole heating system, a micro-CHP, and a gas furnace. The borehole FE model and transfer function model are respectively applied to the optimisation to simulate the borehole wall temperature based on the given discharging heat flux at each time step. The main findings are concluded as follows:

When the borehole transfer function model is employed the optimisation produces approximately the same results compared with the optimisation where the FE model is applied.

The computation time is significantly reduced by applying the borehole transfer function model.

The combined GSHP and borehole system tends to be more stable when the energy hubs are interconnected.

The total energy cost of the community can be significantly reduced by applying the energy hub optimisation scheme.

Future work will be centered on investigating the optimal control policy for combined GSHP and boreholes within energy hub communities on seasonal time scales.

Acknowledgment This work was supported by the CHOICES project of the UK Department of Environment and Climate Change.

References

1. GOV.UK. Exploring how the UK can meet the 2050 emission reduction target using the web-based 2050 Calculator. 2018–06–22, https://www.gov.uk/2050-pathways-analysis

2. Guan X H, Xu Z B, Jia Q S. Energy-efficient buildings facilitated by microgrid. IEEE Transactions on Smart Grid, 2010, 1(3): 243–252 doi:10.1109/TSG.2010.2083705

3. Geidl M. Integrated modeling and optimization of multi-carrier energy systems. Dissertation for the Postdoctoral degree. Zurich: ETH Zurich, 2007

4. Moeini-Aghtaie M, Abbaspour A, Fotuhi-Firuzabad M, Hajipour E. A decomposed solution to multiple-energy carriers optimal power flow. IEEE Transactions on Power Systems, 2014, 29(2): 707–716 doi:10.1109/TPWRS.2013.2283259

5. Shabanpour-Haghighi A, Seifi A R. Energy flow optimization in multicarrier systems. IEEE Transactions on Industrial Informatics, 2015, 11(5): 1067–1077 doi:10.1109/TII.2015.2462316

6. Kienzle F, Ahcin P, Andersson G. Valuing investments in multi-energy conversion, storage, and demand-side management systems under uncertainty. IEEE Transactions on Sustainable Energy, 2011, 2(2): 194–202 doi:10.1109/TSTE.2011.2106228

7. Geidl M, Andersson G. Optimal power flow of multiple energy carriers. IEEE Transactions on Power Systems, 2007, 22(1): 145–155 doi:10.1109/TPWRS.2006.888988

8. Huo D, Liu Y, Gu C H, Blond S L. Optimal flow of energy-hub including heat pumps at residential level. In: Power Engineering Conference, Stoke on Trent, UK, 2015 doi:10.1109/UPEC.2015.7339899

9. Korada N, Mishra M K. Grid adaptive power management strategy for an integrated microgrid with hybrid energy storage. IEEE Transactions on Industrial Electronics, 2017, 64(4): 2884–2892 doi:10.1109/TIE.2016.2631443

10. Sun Q Y, Huang B N, Li D S, Ma D Z, Zhang Y B. Optimal placement of energy storage devices in microgrids via structure preserving energy function. IEEE Transactions on Industrial Informatics, 2016, 12(3): 1166–1179 doi:10.1109/TII.2016.2557816

11. Sanner B, Karytsas C, Mendrinos D, Rybach L. Current status of ground source heat pumps and underground thermal energy storage in Europe. Geothermics, 2003, 32(4–6): 579–588 doi:10.1016/S0375-6505(03)00060-9

12. Adamek F, Arnold M, Andersson G. On decisive storage parameters for minimizing energy supply costs in multicarrier energy systems. IEEE Transactions on Sustainable Energy, 2014, 5(1): 102–109 doi:10.1109/TSTE.2013.2267235

13. Shao C C, Wang X F, Shahidehpour M, Wang X L, Wang B Y. An MILP-based optimal power flow in multicarrier energy systems. IEEE Transactions on Sustainable Energy, 2017, 8(1): 239–248 doi:10.1109/TSTE.2016.2595486

14. Huo D, Le Blond S, Gu C, Wei W, Yu D. Optimal operation of interconnected energy hubs by using decomposed hybrid particle swarm and interior-point approach. International Journal of Electrical Power & Energy Systems, 2018, 95: 36–46 doi:10.1016/j.ijepes.2017.08.004

15. Arnold M, Negenborn R R, Andersson G, De Schutter B. Model-based predictive control applied to multi-carrier energy systems. In: 2009 IEEE Power & Energy Society General Meeting, Calgary, AB, Canada, 2009

16. Moeini-Aghtaie M, Dehghanian P, Fotuhi-Firuzabad M, Abbaspour A. Multi-agent genetic algorithm: an online probabilistic view on economic dispatch of energy hubs constrained by wind availability. IEEE Transactions on Sustainable Energy, 2014, 5(2): 699–708 doi:10.1109/TSTE.2013.2271517

17. Sun Q Y, Han R K, Zhang H G, Zhou J G, Guerrero J M. A multi-agent-based consensus algorithm for distributed coordinated control of distributed generators in the energy internet. IEEE Transactions on Smart Grid, 2015, 6(6): 3006–3019 doi:10.1109/TSG.2015.2412779

18. Dou C X, Yue D, Han Q L, Guerrero J M. Multi-agent system-based event-triggered hybrid control scheme for energy internet. IEEE Access, 2017, 5(99): 3263–3272 doi:10.1109/ACCESS.2017.2670778

19. Sheikhi A, Rayati M, Bahrami S, Mohammad Ranjbar A. Integrated demand side management game in smart energy hubs. IEEE Transactions on Smart Grid, 2015, 6(2): 675–683 doi:10.1109/TSG.2014.2377020

20. Sheikhi A, Bahrami S, Ranjbar A M. An autonomous demand response program for electricity and natural gas networks in smart energy hubs. Energy, 2015, 89: 490–499 doi:10.1016/j.energy.2015.05.109

21. Bahrami S, Sheikhi A. From demand response in smart grid toward integrated demand response in smart energy hub. IEEE Transactions on Smart Grid, 2016, 7(2): 650–658 doi:10.1109/TSG.2015.2464374

22. Sheikhi A, Rayati M, Bahrami S, Ranjbar A M, Sattari S. A cloud computing framework on demand side management game in smart energy hubs. International Journal of Electrical Power & Energy Systems, 2015, 64: 1007–1016 doi:10.1016/j.ijepes.2014.08.020

23. Kennedy J, Eberhart R. Particle swarm optimization. In: IEEE International Conference on Neural Networks, Perth, WA, Australia, 1995 doi:10.1109/ICNN.1995.488968

24. Bozchalui M C, Hashmi S A, Hassen H, Canizares C A, Bhattacharya K. Optimal operation of residential energy hubs in smart grids. IEEE Transactions on Smart Grid, 2012, 3(4): 1755–1766 doi:10.1109/TSG.2012.2212032

25. Houwing M, Negenborn R R, De Schutter B. Demand response with micro-CHP systems. Proceedings of the IEEE, 2011, 99(1): 200–213 doi:10.1109/JPROC.2010.2053831

26. ofgem. About the domestic renewable heat incentive (RHI). 2018–06–22, https://www.ofgem.gov.uk/environmental-programmes/domestic-rhi/about-domestic-rhi

27. Clean Energy Prospector UK Ltd. Owen square community energy project. 2018–06–22, http://www.cepro.co.uk/2015/04/choices-solar-district-heat-study/

28. Mendis N, Muttaqi K M, Sayeef S, Perera S. Application of a hybrid energy storage in a remote area power supply system. In: Energy Conference and Exhibition, Manama, Bahrain, 2011 doi:10.1109/ENERGYCON.2010.5771747

29. Ebbesen S, Kiwitz P, Guzzella L. A generic particle swarm optimization Matlab function. In: 2012 American Control Conference, Montreal, QC, Canada, 2012 doi:10.1109/ACC.2012.6314697

30. Richardson I, Thomson M, Infield D, Clifford C. Domestic electricity use: a high-resolution energy demand model. Energy and Building, 2010, 42(10): 1878–1887 doi:10.1016/j.enbuild.2010.05.023

31. Yao R M, Steemers K. A method of formulating energy load profile for domestic buildings in the UK. Energy and Building, 2005, 37(6): 663–671 doi:10.1016/j.enbuild.2004.09.007

32. Li R, Wang Z M, Le Blond S, Li F R. Development of time-of-use price by clustering techniques. In: 2014 IEEE PES General Meeting, National Harbor, MD, USA, 2014 doi:10.1109/PESGM.2014.6939335